INVESTIGATION OF THE EFFECTS OF SLOPE INSTABILITY AND ROCKFALL USING GEOPHYSICAL AND GEOTECHNICAL APPROACHES: A CASE STUDY FROM TURKEY

JEOFİZİK VE JEOTEKNİK YAKLAŞIMLAR İLE YAMAÇ DURAYSIZLIĞI VE KAYA DÜŞMESİ ETKİLERİNİN İNCELENMESİ: TÜRKİYE'DEN BİR ÖRNEK

Mehmet Bayram [1*], Nuray Alpaslan [2]

[1] *Bayram Engineering and Drilling, Soil Survey Firm, 47000, Mardin*
[2] *Batman University, Faculty of Engineering and Architecture, Department of Civil Engineering, 72100, Batman*

Yayına Geliş (Recieved): 15.10.2020, Yayına Kabul (Accepted):28.12.2020
*Corresponding author

Abstract
In landslide and slope instability studies, geophysical and geotechnical methods are applied together to examine geological problems. Geotechnical methods require more time and cost more when compared to geophysical methods in terms of application. In this study, electric resistivity tomography (ERT), seismic refraction, and geotechnical analysis studies were performed in an area located in the Artuklu district of Mardin Province, Turkey, where slope instabilities and rock falls have occurred previously, in order to determine the physico-mechanical properties, thickness, seismic velocity, and resistivity of the units constituting the slope rubble, and the obtained results were compatible with each other. According to the seismic refraction measurement results, the S-wave velocities of the 1st layer were calculated as 214–243 m/s, and those of the second layer were 622–675 m/s. In the ERT-1, ERT-2, and ERT-3 resistivity models, the unit with an average resistivity value of 180–350 Ωm was determined as marl; the unit with a resistivity value of 450–1100 Ωm was determined as limestone; the unit with a resistivity value of 11–30 Ωm was determined as clay; and the unit with a resistivity value of 35–150 Ωm was determined as slope rubble. The rock quality of the units belonging to the Gercüş Formation was found as very weak due to the fact that the values of the rock quality designation (RQD) varied between 10% and 17%. It was thought that there were stability problems on the slope that were dependent on the lithology due to the heterogeneous feature of the slope rubble unit in horizontal and vertical directions.

Key words: 2D-Electrical resistivity tomography (ERT), Rock quality designation (RQD), Seismic refraction, Slope rubble

Öz
Heyelan ve yamaç duraysızlığı araştırmalarında jeofizik ve jeoteknik yöntemlerin bütünleşik çalışmalar şeklinde uygulanması jeolojik problemleri incelemek için kullanılmaktadır. Uygulanma açısından jeoteknik yöntemler daha çok zaman ve maliyeti gerektirirken, jeofizik yöntemler daha pratik ve ucuz maliyetli olmaktadır. Bu çalışmada, Türkiye'deki Mardin ili Artuklu ilçesi içerisinde daha önce yamaç duraysızlıklarının ve kaya düşmelerinin oluştuğu alandaki, yamaç molozunu oluşturan birimlerin fiziko-mekanik özelliklerini, sismik hızlarını ve özdirençlerini belirlemek amacıyla elektrik özdirenç tomografi (EÖT), sismik kırılma ve jeoteknik analiz çalışmaları yapılmış sonuçlarının birbiriyle uyumlu olduğu saptanmıştır. Sismik kırılma ölçüm sonuçlarına göre birinci tabaka S-dalga hızları (Vs) 214-243 m/sn, ikinci tabaka S-dalga hızları (Vs) 622-675 m/sn olarak hesaplanmıştır. ERT-1, ERT-2 ve ERT-3 özdirenç modelleri içerisinde ortalama 180-350 Ωm rezistivite değerine sahip birim marn, 450-1100 Ωm rezistivite değerine sahip birim kireçtaşı, 11-30 Ωm rezistivite değerine sahip birim kil ve 35-150 Ωm rezistivite değerine sahip birim yamaç molozu olarak belirlenmiştir. Gerçüş formasyonunu oluşturan birimler için kaya kalitesi (RQD) değerleri de % 10 ile % 17 arasında değiştiğinden kaya kalitesi yönünden çok zayıf olarak tespit edilmiştir. Eğimin yüksek olduğu yerlerde yamaç molozu birimininde yanal da ve düşey de heterojen özellik göstermesi sebebiyle litolojiye bağlı çalışma sahasındaki yamaçta stabilite sorunlarının olduğu düşünülmektedir.

Anahtar Kelimeler: 2D-Elektrik rezistivte tomografi (ERT), Kaya kalite göstergesi (RQD), Sismik kırılma, Yamaç molozu

INTRODUCTION

Many different techniques have been used in landslide or slope movement studies in recent years. However, it is difficult to analyze the results of these techniques. Moreover, it is a challenging task to determine the sliding surface, change of groundwater, and instabilities of slopes, rock, and slope rubble through these approaches. Considering these drawbacks, integrated geophysical and geotechnical studies have gained substantial popularity in landslide studies. Many researchers have conducted studies on landslides by using a simultaneous application of geophysical and geotechnical methods (for example, Uyanık and Türker, 2007; Merritt et al., 2014; Syed Baharom Syed et al., 2014; Yordkayhun et al., 2014; Crawford et al., 2015; Ling et al., 2016; Soto et al., 2017; Ullah and Prado, 2017; Rezaei et al., 2018). The landslide studies performed based on geotechnical methods provide more accurate results but require more time and costs (Lopes et al., 2014; Yilmaz and Narman, 2015; Szokoli et al., 2017). At the same time, drilling logs and geological observations are not sufficient to provide structural/geological information regarding the underground hydrological conditions of the landslide mass, and regarding the horizontal continuity of the sliding surface (Mondal et al., 2008). Geophysical methods provide crucial information by which the sliding zone and the physical dimensions of the structure underneath it can be revealed (Bogoslovsky and Ogilvy, 1977). Also, geophysical measurements and interpretations reduce the number of boreholes required to be drilled. Thus, the reduction of unnecessary borehole costs causes the cost of the field study to decrease. The biggest advantage of geophysical methods compared to direct sampling by drilling is that they are less destructive, cheaper, and less dangerous (Gelişli, 2018). Many researchers have studied landslide problems using geophysical methods (for example, Brooke, 1973; Bogoslovsky and Ogilvy, 1977; Cummings and Clark, 1988; Palmer and Weisgarber, 1988; Frasheri et al., 1998; Arndt et al., 2000; Bichler et al., 2004; Gürbüz et al., 2005; Lebourg et al., 2005; Otto and Sass, 2006; Jongsmans and Garambois, 2007; Göktürkler et al., 2008; Sass et al., 2008; Jongmans et al., 2009; Ristic et al., 2012; Choobbasti et al., 2013; Uyanık and Sabbağ, 2013; Uyanık and Çatlıoğlu, 2014; Karslı, 2015; Karslı et al., 2018; Rezaei et al., 2018). Recently, the low cost, fast, and nondestructive electrical resistivity tomography (ERT) method has been widely used for landslide studies (Batayneh and Al Diabat, 2002; Lapenna et al., 2003; Wisen et al., 2005; Drahor et al., 2006; Ravindran and Ramanujam, 2012). Many researchers have also employed the seismic method to determine the features of landslides (Havenith et al., 2000; Al-Saigh and Al-Dabbagh, 2010; Abidin et al., 2012; Özçep et al., 2012; Şenkaya et al., 2020).

The methods applied alone to examine the mass movements in landslide areas can be insufficient at times. Many methods are needed to examine such areas. In the present study, the causes of mass movement in the landslide area were examined by employing rock mechanics experiments and geophysical methods, as well as laboratory experiments performed within the scope of geotechnical analyzes. Previously, a sufficient number of studies have not been conducted on the mass movements that occurred in the study area in the form of rock fall. It is thought that the studies conducted by using integrated methods will improve to the quality of the interpretation that can be taken in the area. Furthermore, it has been observed that conducting integrated studies in the examination of mass movements, which are affected by many factors in landslide areas, and interpreting the results obtained by geophysical methods in association with geotechnical data provides more accurate and reliable results.

GEOMORPHOLOGY OF STUDY AREA

The study area is located in the Artuklu district of Mardin province in Turkey. Figure 1 shows the geographic location of the study area while Figure 2a shows the location of the study area on a 3D satellite image. The average elevation of the study area is about 1083 meters. The study area has a slope range of 20-30%, and 30-50% (Figure 2b) and has a southwest-sloping topography. Its slope in the north is between 30% and 50%, while it is between 20% and 30% in the south. Depending on the structure of the soil in steep slopes, the soil may move in the slope direction and cause landslide to form. Although the highest elevation is 1090 meters and the lowest elevation is 1048 meters in the study area, there are steep slopes formed as a result of material removal.

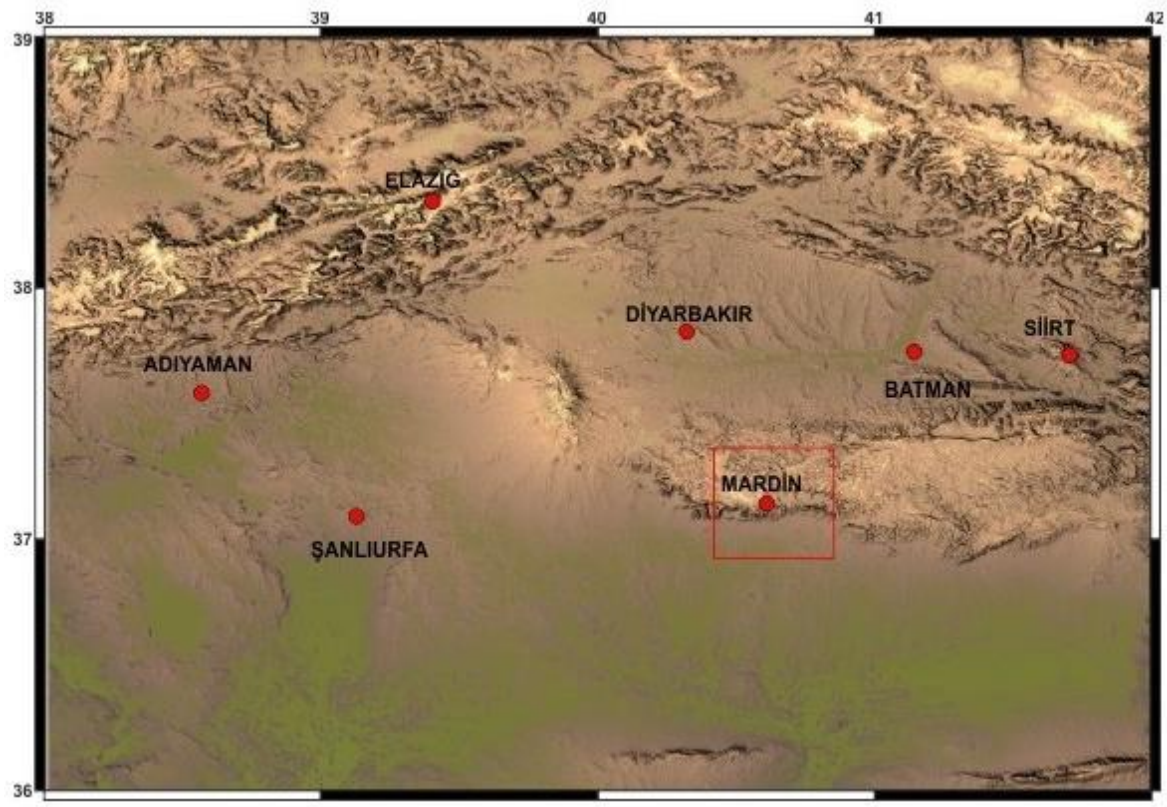

Figure 1. The geographic location of the study area

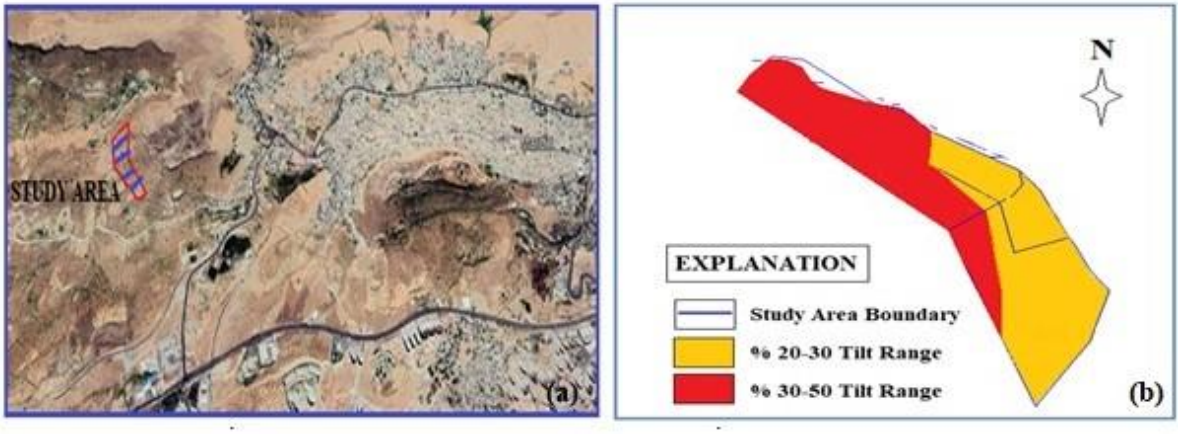

Figure 2. a) 3D satellite image of the study area, **b)** The slope map of the study area

Figure 3 shows that the study area and its immediate surrounding areas are geologically characterized by the Gercüş formation, Upper Miocene units on the Midyat formation with an incompatible angle, slope rubbles, and late Plio-Quaternary units represented by alluviums. There are metamorphosed limestones, late Eocene limestones, and alluvium in this region. The Adıyaman Group is represented by the Karaboğaz and Sayındere formations.

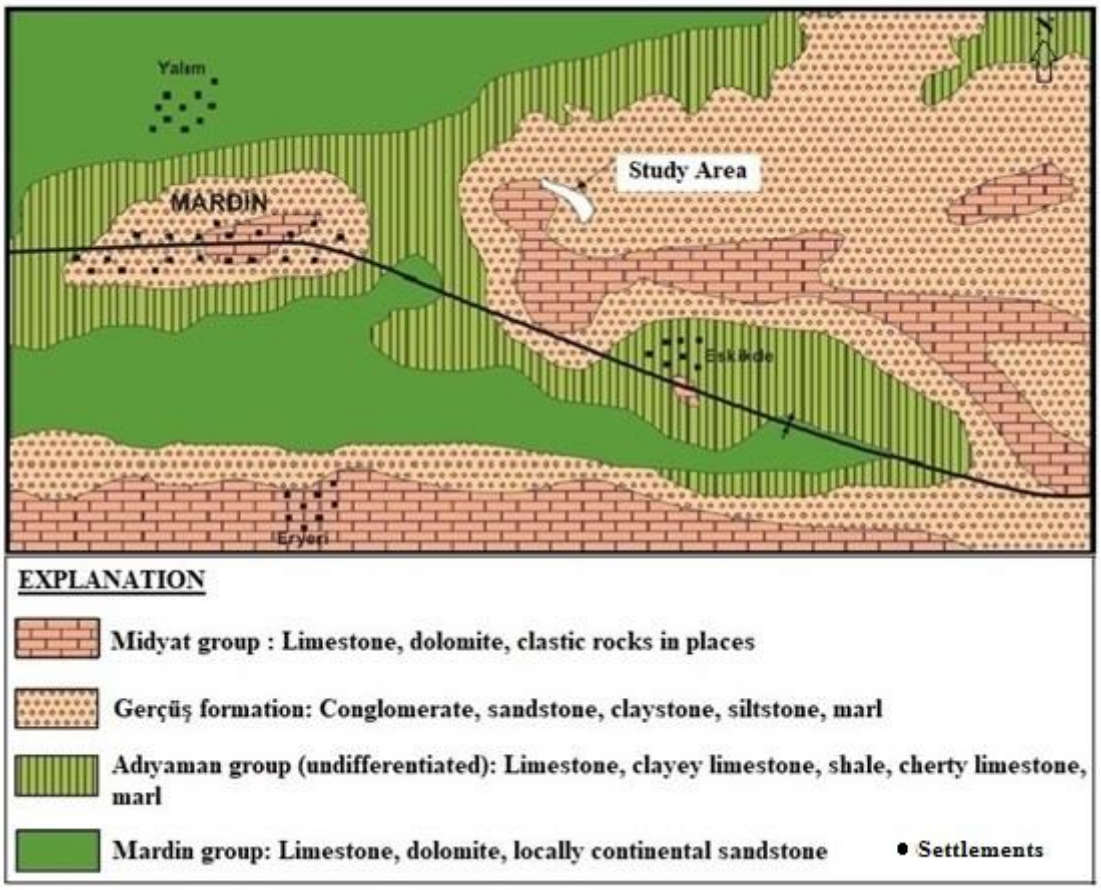

Figure 3. General geology map of the study area and its surrounding areas (map scale=1:100,000) (adopted from MTA)

The limestone units (Figure 4a) are located in the shape of a hat in the peak sections of the slope in the eastern part of the study area. There are large and small rock blocks (Figure 4b) separated from the limestone units. This suggests that a faulted-fissured structure exists in the study area due to the atmospheric conditions and the effects of tectonic stresses. The blocks are also suspended on the slope because of the effect of gravity. Moreover, soils containing limestone can easily be weathered. The separations and falls can take place due to this weathering. Rockfalls generally occur due to the type, weathering, and strength of the geological unit, and weathering of crack surfaces. The mechanism of these falls can be explained by the blocky geological structure of slope rubble material or by the underground water conditions of the residual units. It can also be explained by foot carvings in steep topographic slope conditions, the fall of hydrostatic pressure depending on freezing-thawing effects, and the end of the movement in the levels where the slope is influential.

Figure 4. a) Close-up view and **b)** long-distance view of the study area

FIELD INVESTIGATIONS

Geotechnical investigations

In the study area, six geotechnical boreholes with a depth of 90 meters (Figure 5; BH-1, BH-2, BH-3, BH-4, BH-5, BH-6) were drilled in an area of 48.120 m^2 acres to determine the physical and mechanical properties of the sliding material as well as the engineering properties of the soil. The field observations and drilled geotechnical boreholes indicated that the geology of the study area consisted of the slope rubble on the top followed by units of the Gercüş formation. The dominant units in the study area were slope rubble and the Gercüş formation. The units of slope rubble are mainly formed from low silty pebbled clay, which occasionally contains limestone blocks. However, the units of the Gercüş formation are composed of greenish cream, grayish beige, and variegated claystone, clayey marl, marl, and grayish-white clayey limestone, and partly limestone blocks. The units belonging to slope rubble were classified as soil while the units belonging to the Gercüş formation were classified as rock. In the drilled boreholes, units belonging to slope rubble were observed at a depth of 2.10-3.70 meters, and units belonging to the Gercüş formation were observed at a depth of 3.70-15.00 (see Table 1). Also, a standard penetration test (SPT) was carried out on the upper levels of the slope rubble unit, having no pebbled and blocky structure, at every 1.5 meters in each borehole (see Table 2). In the continuation of the study, the required experiments were conducted to determine the physico-mechanical properties of core samples obtained from the geotechnical boreholes. The calculated geotechnical parameters of the units belonging to slope rubble were as follows (see Table 3): a natural unit volume weight of 1.84 g/cm^3, a cohesion of 0.64 kg/cm^2, and an internal friction angle of 6°. In the consolidation test results of the samples obtained from the slope rubble unit, the liquid limit (LL) values were determined to be between 53.2% and 62.4%, and the plasticity index (PI) values were determined to be between 28.8% and 36.7%. It was also found that the clays had a “high” swelling degree according to Holtz and Gibbs (1956) and Chen (1975) (see Table 4).

Table 1. Geological description of the core samples obtained from the boreholes

Depth (m)	Geological description of the units
2.10-3.70	Slope rubble
3.70-15.00	Gercüş formation

Table 2. The standard penetration test (SPT) results obtained from the borehole studies

Borehole No.	Depth (m)	SPT values				Formation
		0-15 cm	15-30 cm	30-45 cm	N30	
BH-1	1.50-1.95	5	8	9	17	**Slope rubble**
BH-2	1.50-1.95	9	12	12	24	
BH-3	1.50-1.95	6	11	10	21	
BH-4	1.50-1.95	7	10	18	28	
BH-5	1.50-1.95	8	8	10	18	
BH-6	1.50-1.95	9	R	R	R	

Table 3. Geotechnical parameters of the core samples obtained from the slope rubble boreholes

Geological unit	Natural unit volume weight (g/cm^3)	Cohesion (kg/cm^2)	Internal friction angle (°)
Slope rubble	1.84	0.64	6

Table 4. The swelling potential of the slope rubble units based on the liquid limit (LL) and plasticity index (PI) (UD: Undisturbed sample, CH: High plasticity clay)

Borehole No.	Sample type	Depth (m)	Atterberg limits				Soil class
			Liquid limit (LL) %	Swelling degree (Chen, 1975)	PI %	Swelling degree (Holtz and Gibbs, 1956)	
BH1	SPT	1.50-1.95	53.6	High	29.1	High	CH
BH2	SPT	1.50-1.95	58.2	High	33.1	High	CH
BH3	SPT	1.50-1.95	57.1	High	31.8	High	CH
BH3	UD	2.00-2.45	62.4	High	34.5	High	CH
BH4	SPT	1.50-1.95	59.6	High	36.7	High	CH
BH4	UD	3.00-3.45	59.9	High	34.6	High	CH
BH5	SPT	1.50-1.95	55.7	High	33.2	High	CH
BH5	UD	2.80-3.30	58.1	High	31.6	High	CH
BH6	SPT	1.50-1.95	53.2	High	32.1	High	CH
BH6	UD	2.50-3.00	52.3	High	27.0	High	CH

Point loading experiments were carried out on the samples obtained from the geotechnical boreholes drilled at the Gercüş formation. Uniaxial compressive strengths were calculated from the point load indexes obtained from the point loading experiments. Also, the point loading strengths of the units were calculated according to Gupta and Rao (1998) as follows (see Table 5): limestone (Is_{50} = 8.7 kg/cm^2), claystone (Is_{50} = 14.0 kg/cm^2), marl (Is_{50}=21.6 kg/cm^2) and clayey limestone (Is_{50}=26.5 kg/cm^2), which are classified respectively as very low, low, and medium strength. The corresponding uniaxial compressive strengths are classified as very low and low strength. The equation can be given as follows:

$$\mathbf{UCS = 12 * I_{s(50)}}$$

where UCS represents unconfined compressive strength (kg/cm^2) and $I_{s(50)}$ Point load strength (kg/cm^2)

These findings are shown in Table 6. According to the ISRM (1978), the units of the Gercüş formation are classified as follows: limestone is classified as highly weathered (W4); claystone-marl, clayey

limestone, and claystone are classified as moderately weathered (W3); and clayey marl is classified as highly weathered (W4) (see Table 7). Because the limestone unit had a faulted-fissured structure and had small melting gaps, a higher degree of weathering was observed in this unit compared to other units. In light of the cores obtained from the boreholes, it was found that the rock quality designations (RQDs) of units belonging to the Gercüş formation were in the very weak range and these RQD values varied between 10% and 20% (see Table 8). A regular variation was found when the RQD values were evaluated together against the depth of sampling

Table 5. Classification of rocks based on the results of the point loading experiments (Bieniawski, 1975)

Rock class	**Uniaxial compressive strength (kg/cm^2)**	**Point load strength (kg/cm^2)**
Very high strength	>2000	>80
High strength	1000-2000	80-40
Medium strength	**500-1000**	**40-20**
Low strength	**250-500**	**10-20**
Very low strength	**<250**	**<10**

Table 6. Point load strength and uniaxial compressive strength of units belonging to the Gercüş formation

Point load strength (kg/cm^2)	**Strength classification**	**Unconfined compressive strength (kg/cm^2)**	**Strength classification**	**Lithology (Gercüş formation)**
8.7	Very low	194.4	Very low strength	Limestone
14.0	Low	168	Very low strength	Claystone
21.6	Low	231.6	Low strength	Marl
26.5	Medium	318	Low strength	Clayey limestone

Table 7. Determination of rock mass quality based on rock quality designation (RQD) (Deere and Miller, 1966)

Rock quality designation (RQD %)	**RQD classification**
0-25	Very poor (Completely weathered rock)
25-50	Poor (weathered rocks)
50-75	Fair (Moderately weathered rocks)
75-90	Good (Hard Rock)
90-100	Very Good (Fresh rocks)

Table 8. Rock quality designation (RQD) and weathering degree of the units belonging to the Gercüş formation

Borehole	Rock quality designation (RQD) (%)	Rock quality	Weathering degree	Symbol	Lithology (Gercüş formation)
BH-1	**10**	Worse	Highly weathered	W4	Limestone
BH-1	**15**	Worse	Moderately weathered	W3	Claystone-marl
BH-1	**13**	Worse	Moderately weathered	W3	Clayey limestone
BH-2	**12**	Worse	Moderately weathered	W3	Claystone
BH-3	**16**	Worse	Highly weathered	W4	Clayey marl
BH-5	**20**	Worse	Moderately weathered	W3	Claystone

Geophysical investigations

Electrical resistivity measurement is an effective method actively used to determine the underground conductive structures, layers thickness, and water content properties of underground units. This method is based on the principle of calculating the apparent resistivity values by measuring the potential differences, in the units of the ground with pair of potential electrodes, which is created by a pair of current electrodes. With the developments in computer programs and equipment more than a couple of decades, the electrical resistivity measurement allows for an easier analysis of horizontal and vertical changes in electrical mapping by providing better 2D and 3D modeling (Griffiths and Turnbull, 1985; Griffiths et al., 1990; Li and Oldenberg, 1992; Loke and Barker, 1996; Dahlin and Bernstone, 1997; Candansayar and Başokur, 2001; Kurtulmuş, 2003; Dahlin and Zhou, 2004). More detailed modeling of the underground structures can be provided especially with multi-electrode systems that can collect data in a fast and practical manner. It is possible to provide easy and practical information about the resistivity structure of the underground both vertically and horizontally. This is procured using multi-electrode electrical resistivity imaging, which can be changed automatically to obtain drilling-profile measurements along one direction. The method offers the benefits of vertical electrical sounding and profile measurement techniques (Van Overmeeren and Ritsema, 1988; Griffiths et al., 1990; Dahlin, 1996). Electrical resistivity measurement method is widely used in engineering studies. Especially in landslide and slope insensitivity studies, the relationship between resistivity, water content and electrical conductivity are important parameters in resistance to slipping. Many researchers have done various studies on this subject. Electrical conductivity of the extracted soil solutions have been studied vigorously (Campbell et al., 1948; Larsen and Widdowson, 1965; Rhoades et al., 1976; Rhoades et al., 1990). Another working group includes on-site measurements of electrical conductivity of soils, rocks and sediments by various geophysical methods (Pozdnyakova et al., 1996; Pozdnyakova, 1999; Özçep et al., 2009, 2010). In the study area, 2D ERT images were created using tomography measurements made in three profiles (Figure 5) with a profile length of approximately 123 meters. The electrical resistivity distribution of the units constituting the slope was studied by using the electrical conductivity differences of the underground structures located throughout the area in horizontal and vertical directions. The resistivity field data were acquisited by the 8-channel 84-electrode AGI R8 device (Figure 6a) and analyzed by the EarthImager 2D program. EarthImager 2D discretized the subsurface model into a finite element grid. The finite element model of electrical resistivities is automatically modified through an iterative process, so that the model response converges towards the measured data (Loke and Barker, 1996). Loke and Barker (1996a,b) used a quasi-Newton method to estimate the partial derivatives to reduce the computing time. For the nonlinear inversion of the simulated data, EarthImager 2D's smooth model inversion algorithm was used, which was based on Constable et al. (1987) work. The root mean square (RMS) is a measure of it fitness between measured apparent resistivities and the apparent resistivities of the model response from the inverted resistivity (Bernstone et al., 2000).

In the electrical resistivity studies, the electrode spacing was chosen to be 3 meters and Schlumberger electrode array was used with 42 electrodes as shown in Figure 6b. Therefore, different interpretations were made about the approximate cover thickness, and layers depths on 2D ERT sections obtained from the three surveying profiles as shown in Figure 5 (purple lines-ERT-1.2.3).

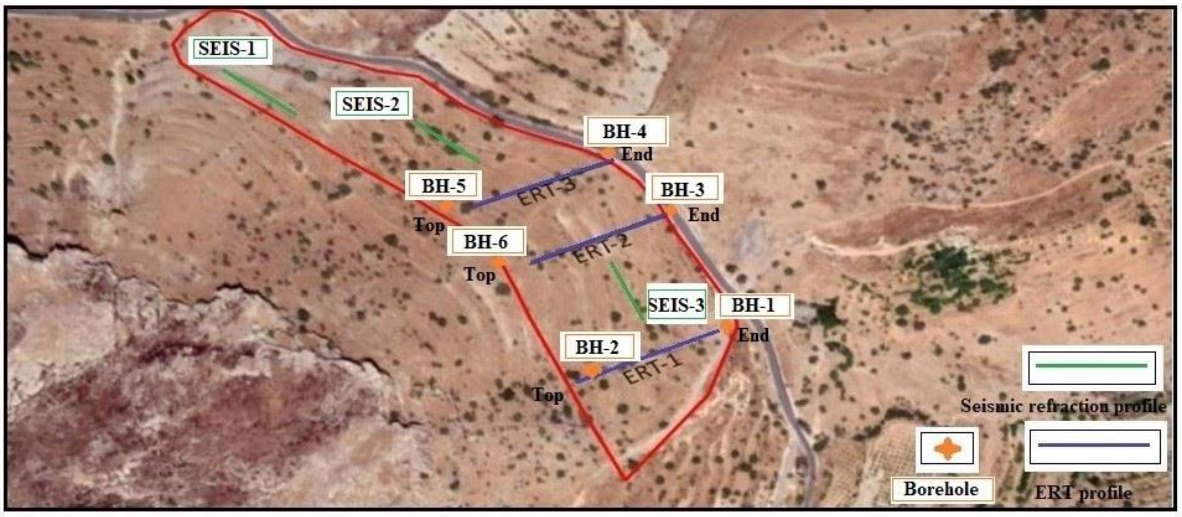

Figure 5. The measurement directions of the electrical resistivity tomography and seismic profiles and the locations of the geotechnical boreholes in the study area

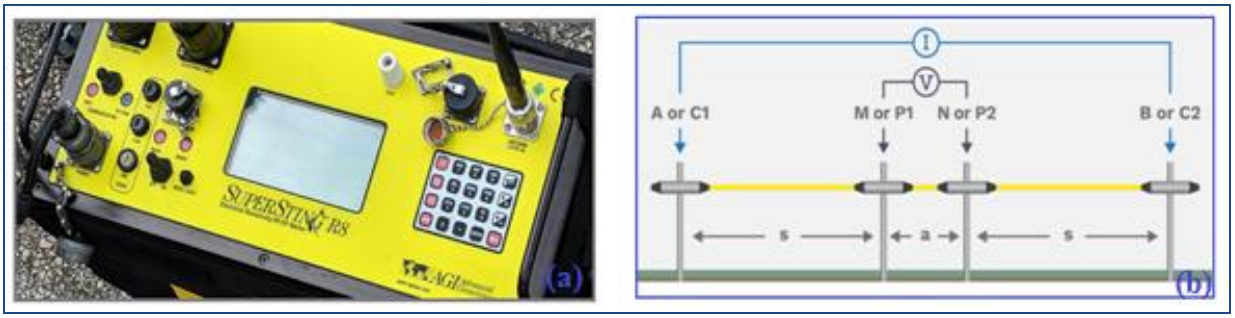

Figure 6. a) SuperSting R8 resistivity device, **b)** Schlumberger electrode array (https://www.agiusa.com)

Seismic refraction, another method used in this study, is based on analysis of the wave arrival times (Figure 7a). This is performed by measuring the travel time of the seismic waves in the superficial layer and their rapid refractions by breaking through the substrates, with the help of geophones placed on the ground. With this method, a source pulse is sent to the ground by using one of the impulsive seismic sources, a sledgehammer. The seismic P-(primary/compressional wave) and S- (secondary/shear wave) velocities of the underground layers are determined by seismic receivers that record the seismic waves reproduced from this source. Seismic refraction profile measurements (green lines, SEIS-1, SEIS-2, SEIS-3) (Figure 5) were evaluated to determine the seismic velocities of the units constituting the slope in the study area. In seismic refraction measurements, the total line length was defined as 57.5 meters, while geophones were placed at intervals of 5 meters with an offset distance of 2.5 meters, and approximately 30 meters of the depth was reached. A 12-channel RAS24 seistronix seismic device (Figure 7b) was employed during the field studies. Since noise separation and analog and digital filtering are done automatically in monitoring the signal during the measurements, a high signal-to-noise ratio was achieved while consuming minimal power. The system consisted of a triggered sledgehammer, twelve horizontal and twelve vertical geophones, and special connection units, which can select the sampling interval through a computer. The hits on the 6-kg steel plate by the sledgehammer were used as a seismic wave source and a 14-Hz P geophone and a 14-Hz S geophone were used to measure the refracted waves. The measurements in the field were made and recorded using Seismodule Controller Software (version 9.28). Also, the recorded seismic refraction measurements were analyzed by SeisImager software (version 2.8.0.1).

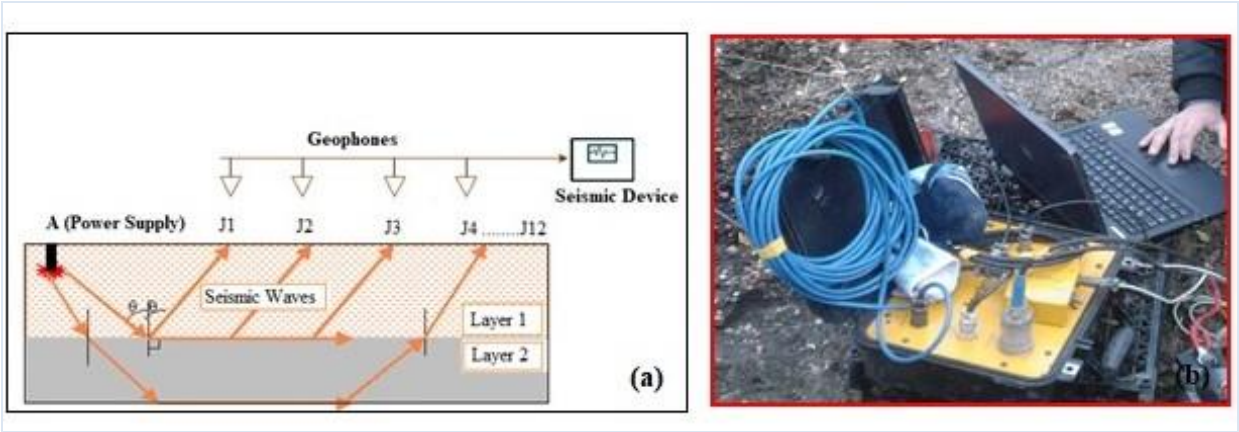

Figure 7. a) A simple image of seismic refraction method including wave path and geometry, **b)** 12-channel RAS24 seistronix seismic device (http://www.seistronix.com/)

RESULTS

To determine the potential slope effects and rockfall risks, ERT measurements (Figure 5) were conducted on a NE-SW line in three profiles (ERT-1, ERT-2, ERT-3), which are 123 meters long each and are parallel to each other with equal average elevation levels. The 2D ERT results (Figure 8a, Figure 8b, Figure 8c) for the ERT-1 profile indicated that the unit represented with blue in the inverse solution model section was the claystone unit, with an average electrical resistivity of 38–90 Ωm; the unit represented with green was the marl unit, with an average electrical resistivity of 180–350 Ωm; and the unit represented with red was the limestone unit, with an average electrical resistivity of 450–1100 Ωm (Figure 8c). The dominant units in this section are as follows: the limestone unit is the prevalent unit in the lower elevations of the left side of the section, while unit transitions from marl unit to claystone unit were prevalent at the surface of the right side of the section. The areas indicated in blue in the upper elevations represent the clay unit, while there is a more massive and compact claystone unit, indicated in blue, towards the lower elevations. Transitions were observed between the limestone, indicated in red, in the higher elevations and the clayey limestone unit, indicated in yellow, in the lower elevations. In the inverse solution process, the number of iterations was 6 and the RMS error rate was 8.97%. It is consider that the small melting gaps observed in limestone units may increase in rainy seasons and cause a rockfall, debris flows and mudflows to occur. The 2D ERT results (Figure 9a, Figure 9b, Figure 9c) obtained for the ERT-2 profile, which was the second profile, suggested that the unit represented with blue in the inverse solution model section was the clay, with claystone in the lower elevations, with an average electrical resistivity of 6–30 Ωm; the unit represented with green is the slope rubble unit with an average electrical resistivity of 35–200 Ωm; and the unit represented with red is the limestone unit with an average electrical resistivity of 750–3600 Ωm. The dominant units in this section were clayey blocky slope rubble materials in the upper levels, while blocky slope rubble materials were more compact in the lower elevations. Units indicated with blue represent the claystone units (Figure 9c) in the lower levels. In the inverse solution process, the number of iterations was 7 and the RMS error rate was 8.96%. Because the slope rubble unit had a heterogeneous structure, it varied in the horizontal and vertical directions. Due to the high swelling degree and strong water content properties of the clay belonging to the slope rubble unit, it can make sliding easier in the rainy seasons by accumulating surface water at this border and bringing an additional load to the mass. The increase in pore pressure, hence, the decrease in mean normal effective stress and finally, more likelihood for rock/soil shear failure. The 2D ERT results (Figure 10a, Figure 10b, Figure 10c) obtained for the ERT-3 profile, which was the third profile, showed that the unit represented with blue in the inverse solution model section was the clay, with claystone in the lower elevations, with an average electrical resistivity of 11–30 Ωm; the unit represented with green was the slope rubble unit with an average electrical resistivity of 35–150 Ωm; and the unit represented with red is the blocky slope rubble unit with an average electrical resistivity of 180–400 Ωm. The dominant units in this section were clayey blocky slope rubble materials (Figure 10c) in the upper levels while blocky slope rubble materials were more compact in the lower elevations. Units indicated with blue represent the claystone units in the lower levels. Legend intervals in the ERT models (Figures 8a–8c, 9a–9c, and 10a–10c)

were created using different values in order to define the units more clearly.

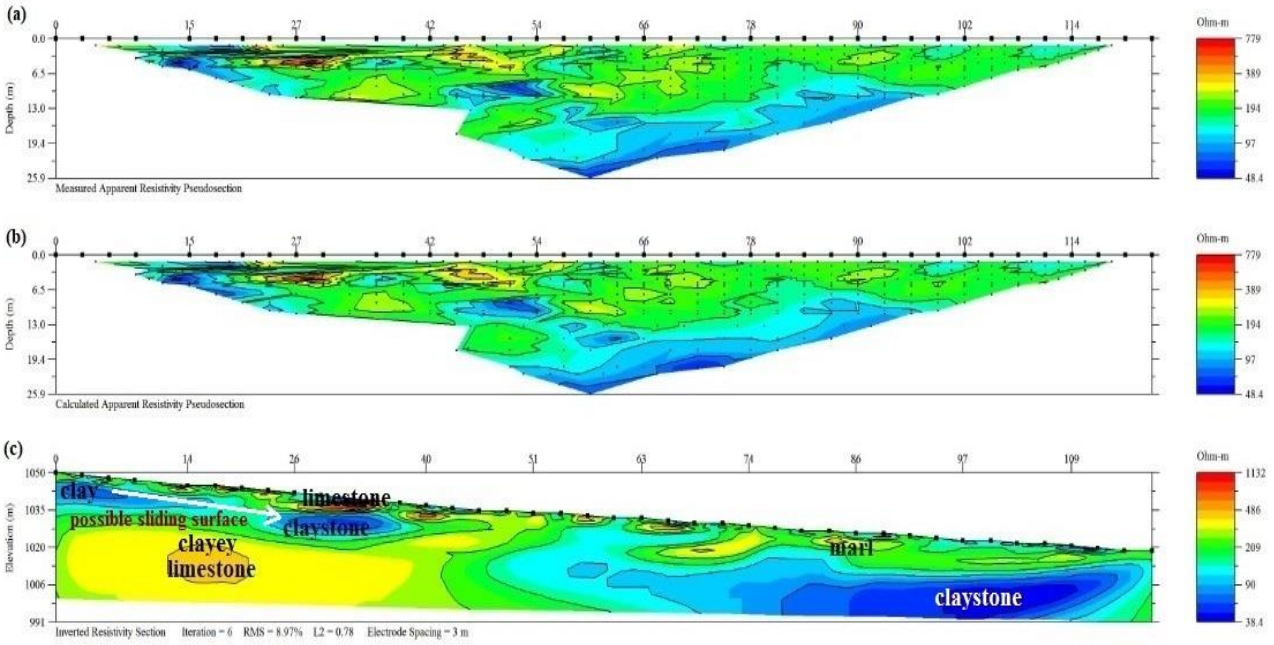

Figure 8. a) Two-dimensional (2D) underground model of the ERT-1 profile obtained by multi-electrode resistivity tomography, **b)** apparent resistivity section calculated by inverse solution, **c)** transformed resistivity model section

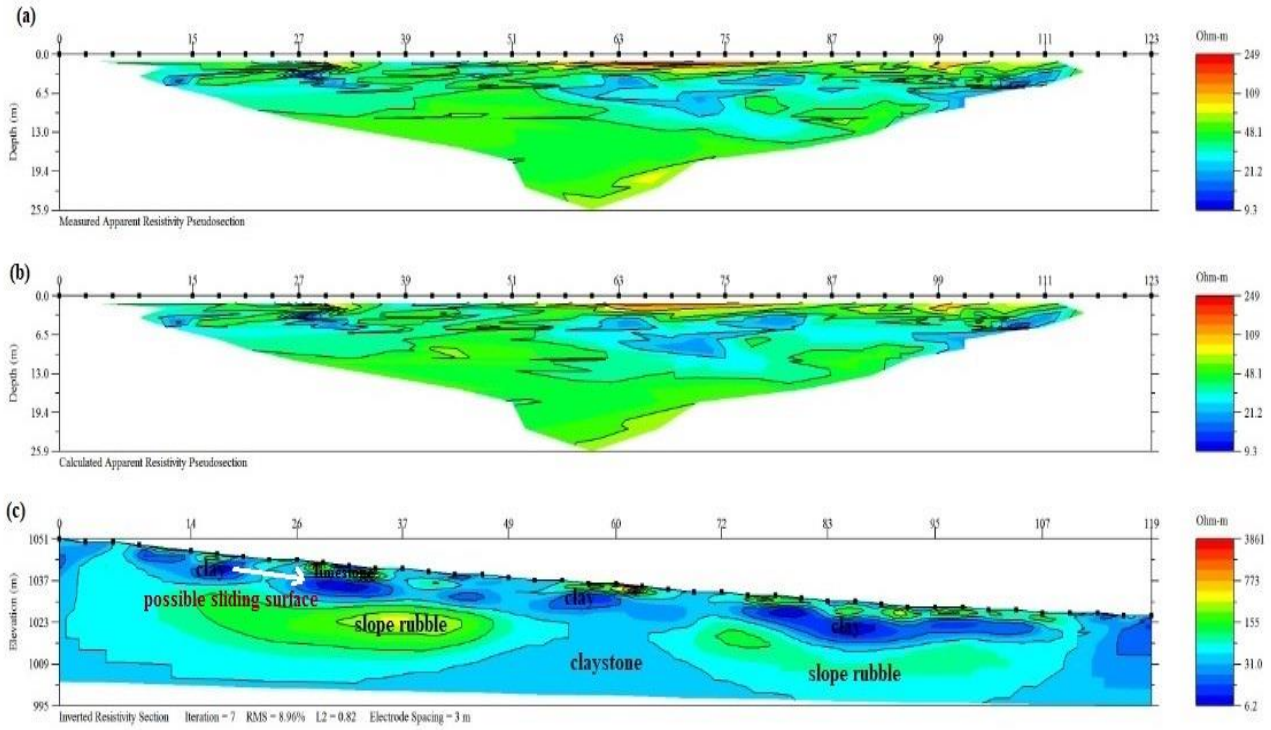

Figure 9. a) Two-dimensional (2D) underground model of the ERT-2 profile obtained by multi-electrode resistivity tomography, **b)** apparent resistivity section calculated by inverse solution, **c)** transformed resistivity model section

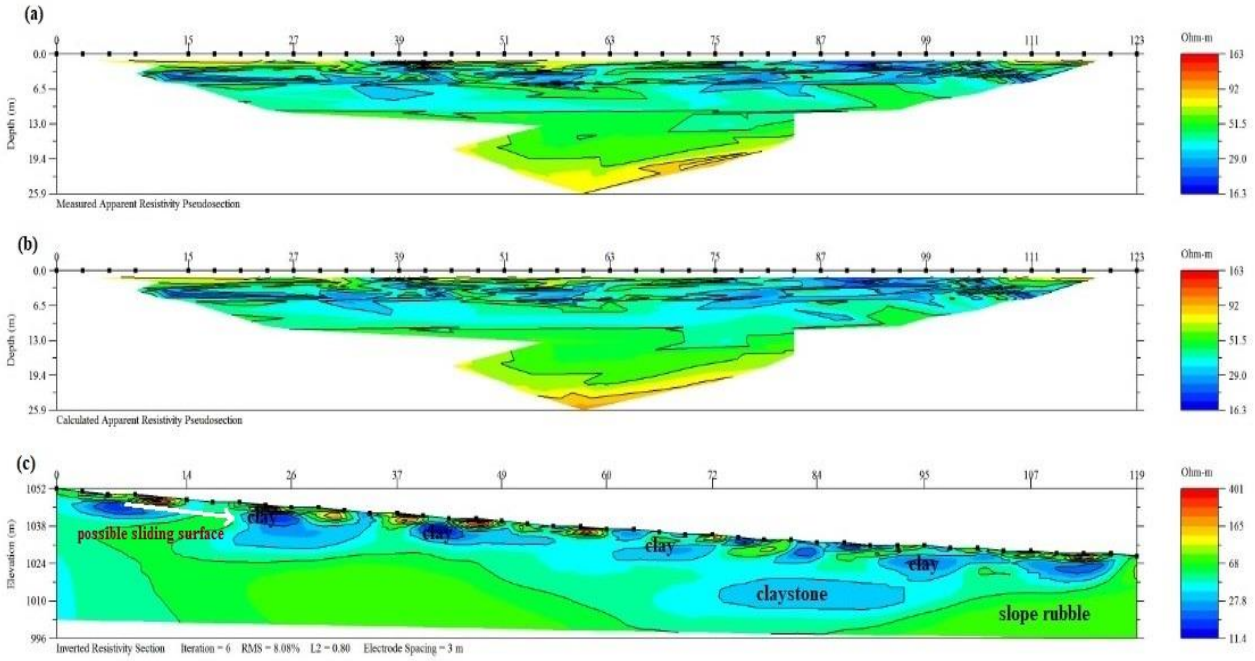

Figure 10. a) Two-dimensional (2D) underground model of the ERT-3 profile obtained by multi-electrode resistivity tomography, **b)** apparent resistivity section calculated by inverse solution, **c)** transformed resistivity model section

According to the seismic refraction measurements performed on three different profiles in the study area (Figure 5), and pursuant to the measurements made on the SEIS-1 Profile, the P-wave velocity of the 1st layer was calculated as Vp = 513 m/s and the S-wave velocity was calculated as Vs = 243 m/s. These same velocities were calculated in the 2nd layer as Vp = 1200 m/s and Vs=675 m/s. According to the measurements performed on the SEIS-2 profile, the same velocities were calculated in the 1st layer as Vp = 467 m/s and Vs = 214 m/s, and in the 2nd layer as Vp = 1187 m/s and Vs = 622 m/s. In the measurements performed on the SEIS-3 profile, these same velocities were found in the 1st layer as Vp = 541 m/s and Vs = 226 m/s, and in the 2nd layer as Vp = 1237 m/s and Vs = 643 m/s. According to the geological units, in the 1st layer, the S-wave velocities were between 214 and 243 m/s, and between 622 and 675 m/s in the 2nd layer. In the 1st layer, P-wave velocities were determined as 467-541 m/s and in the second layer as 1187-1237 m/s.

DISCUSSION

The following units were represented in the ERT-1, ERT-2, and ERT-3 resistivity models: claystone with the electrical resistivity of 38–90 Ωm, marl with 180–350 Ωm, limestone with 450–1100 Ωm, clay with 11–30 Ωm, slope rubble with 35–150 Ωm, and blocky slope rubble with 180–400 Ωm. It can be observed that clay and claystone units, which are sedimentary rocks with multiple cavities and high water content, had smaller resistivity values. Although the possible sliding surface in the ERT-2 and ERT-3 resistivity models (Figure 9c and Figure 10c) was not clear, the presence of clay soil and fill slope in the areas close to the surface and in the areas where the topographic slope is steep indicated that surface sliding may took place along the topographic slope.

According to the obtained S-wave velocities, the 1st layer was generally loose and the strict was very low. Therefore, surface sliding can occur along the slope when the soil becomes saturated with water. The shear wave velocities (Vs30) obtained for the three layers in the study area were between 508 and 548 m/s. The measurement of the S-wave (shear wave) velocity is the most important issue in determining the mechanical properties of the soil such as the shear strength. It is well known shear wave velocities are generally low in soft soils that have low shear strength. That is, the soils that have small shear wave velocities had a loose structure. Geological units with shear wave

velocities greater than 700 m/s are called engineering base. These can be defined as firm or hardened rocks, highly strict sand, pebbles, and stiff clay. If the horizontal (shear) wave velocities are between 300 and 700 m/s, they represent weathered rocks or strict sand, pebbles, very stiff clay, and silty clay soils. The shear wave velocities of highly weathered rocks and medium strict sand, gravel, stiff clay, and silty soils are about 200–300 m/s. Geological units with shear wave velocities of less than 200 m/s are soft, thick alluvium layers, loose sand, soft clay, and silty clay, which are found in areas with a high groundwater level (BSSC, 1997).

According to the soil profiles in the study area, in the direction of the BH-1 and BH-2 boreholes (A-B length section) (Figure 11), P wave velocity (Vp) was calculated as 541 m/s and S wave velocity (Vs) as 226 m/s in the slope rubble unit, while P wave velocity (Vp) was calculated as 1237 m/s and S wave velocity (Vs) as 643 m/s in the unit belonging to the Gercüş Formation. In the direction of the BH-3 and BH-5 boreholes (C-D length section) (Figure 11), P wave velocity (Vp) was calculated as 467 m/s and S wave velocity (Vs) as 214 m/s in the slope rubble unit, while P wave velocity (Vp) was calculated as 1187 m/s and S wave velocity (Vs) as 622 m/s in the unit belonging to the Gercüş Formation. In the geotechnical analyses carried out, rock quality designation (RQD) was calculated as 10-15% and point loading strength (Is_{50}) as 8.7 and 17.8 kg/cm^2 for borehole BH-1, while RQD was 10-17% and Is_{50} was 12.5 and 23.7 kg/cm^2 for BH-2, RQD was 14-16% and Is_{50} was 11.1 and 22.9 kg/cm^2 for BH-3, and RQD was 12-20% and Is_{50} was 8.4 and 26.5 kg/cm^2 for BH-5 (Figure 12a, 12b and Table 9). According to the Turkish Building Earthquake Code (2018), the soil type (ST) of the rock units belonging to the Gercüş Formation was determined as highly dense sand and highly stiff clay or weathered, highly fissured weak rocks. Furthermore, according to the results of geotechnical analyses, the rock quality of the units belonging to the Gercüş Formation was determined as very weak due to the fact that the values of RQD varied between 10% and 20%. Moreover, the Is_{50} values of this unit were in the very low-low class as they ranged between 8.5% and 26.5%. This shows that the rock unit of this formation is weak and has low strength. Low values were obtained for the resistivity and seismic velocities of the units in the study area by geophysical methods and the RQD and Is_{50} values determined via geotechnical analyses. It was observed that conducting integrated studies and interpreting the results obtained by geophysical methods together with geotechnical data in the examination of mass movements, which are affected by many factors, supported each other. Additionally, the slope rubble unit in the study area, which has a heterogeneous structure and different characteristics in lateral and vertical directions, and the limestone unit, which dominates the peak parts of the slope at high elevations and demonstrates a faulted-fissured structure, are separated from the bedrock and fall due to the effect of gravity and atmospheric conditions. The mechanism of these falls can be explained by the blocky geological structure of slope rubble material or the underground water conditions of the residual units, high topographic slope conditions, the falling of hydrostatic pressure depending on freezing-thawing effects, and the ending of the movement in the levels where the slope has an effect.

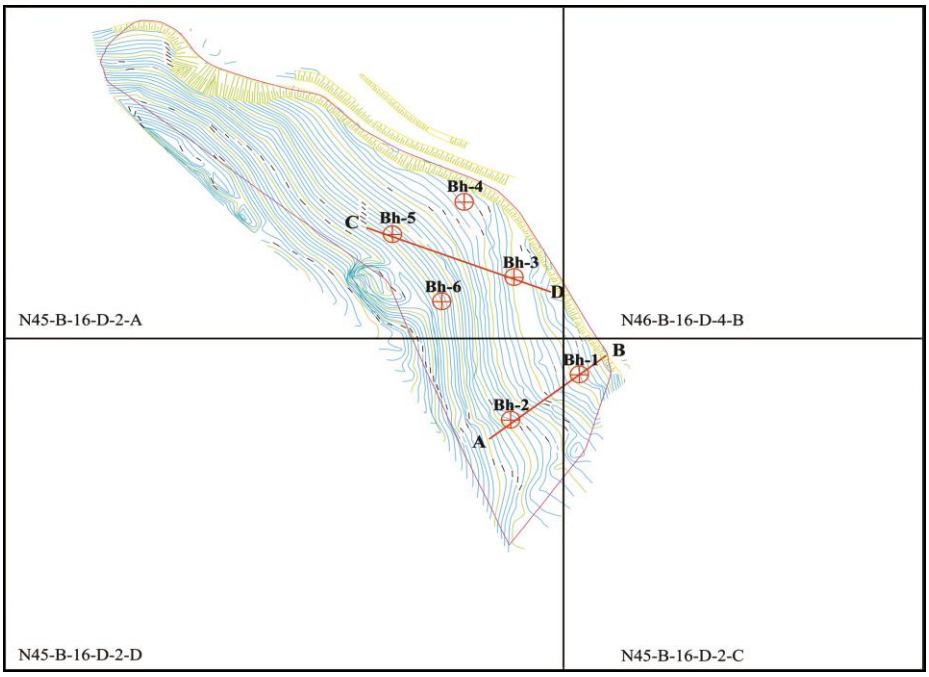

Figure 11. A-B and C-D sections of the study area

Table 9. Geophysical and geotechnical parameters

Borehole No.	**SPT values (N30)**	**Rock quality designation (RQD) (%)**	**Point load strength (I_{S50})(kg/cm^2)**	**Seismic Velocity (m/sn)**	
				Slope Rubble	**Gerçüş Formation**
BH-1	17	% 10-15	8.7-17.9	Vp=541 Vs=226	Vp=1237 Vs=643
BH-2	24	% 10-17	12.5-23.7		
BH-3	21	% 14-16	11.1-22.9	Vp=467 Vs=214	Vp=1187 Vs=622
BH-5	18	% 12-20	8.4-26.5		

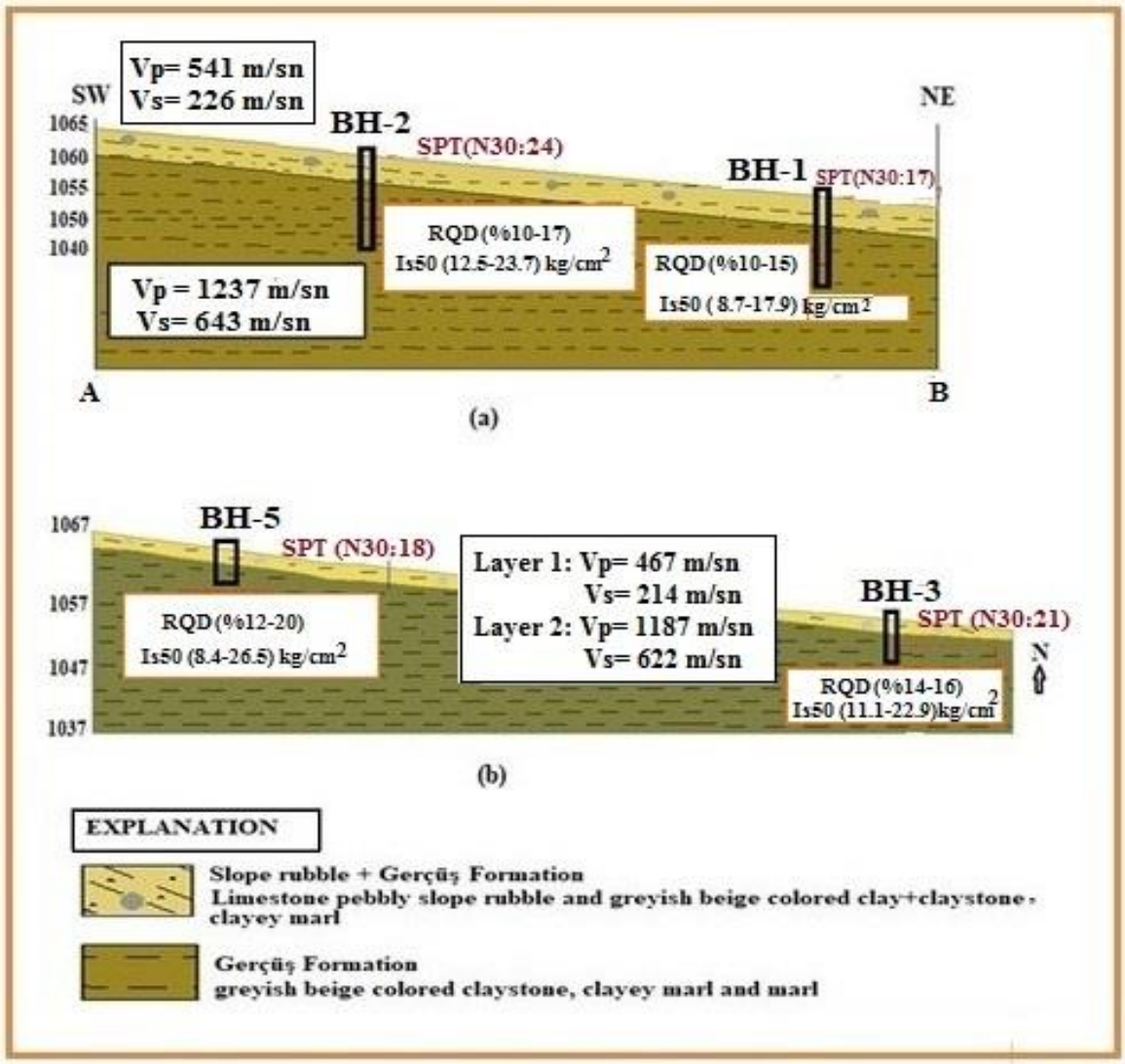

Figure 12. a) A-B cross section of the study area, **b)** C-D cross section of the study area

CONCLUSION

The main emphasis of this study was on the importance of making evaluations by the simultaneous use of geophysical and geotechnical methods to obtain more reliable results in solving problems in geological structures that are difficult to interpret. The properties of the geological units of the study area and the effects of the slope instability and rockfall were investigated by conducting geotechnical analyses along with the ERT and seismic refraction methods, which are both geophysical methods. Therefore, it was observed that slope instability and rockfall problems have frequently occurred, and moving blocks have progressed to a certain distance. When the ERT-1 and ERT-2 resistivity models and the P-and S-wave velocities of the SEIS-3 profile located between those two models were evaluated together, it was observed that the resistivity and seismic velocity values of the material in the slope rubble unit, which was approximately 4 m thick, were low. Therefore, this unit was considered as a very loose unit. Thus, the risk of falling and overturning along the slope with the blocks separating from the bedrock was predicted to be serious. Seismic P-wave velocities of the slope rubble unit from 2.10 to 3.70 m in the BH-1 and BH-2 geotechnical boreholes were found as 467–541 m/s and the S-wave velocities were found as 214–243 m/s.

Seismic P-wave velocities were calculated between 1187 and 1237 m/s and the S-wave velocities were between 622 and 675 m/s in the Gerçüş Formation unit, which was also determined by the geotechnical boreholes drilled. Likewise, in the rock mechanics

experiments conducted on the rocks forming this formation, the RQD values were typical of "very low strength, highly weathered, and poor" rocks. This originated from the fact that the material had a faulted-fissured and fractured structure and contained large and small discontinuity surfaces. However, the consolidation test revealed that the dominant slope rubble unit in the study area had a high swelling degree. This showed that the clays of this unit in the study area had water content and impermeable properties.

Furthermore, the slope rubble unit varies in lateral and vertical directions due to its heterogeneous structure. Therefore, it is important to transport building loads or foundations to homogeneous levels, or to pay attention to choosing the appropriate foundation type. It is thought that it would be appropriate to reclaim the big rock blocks in the study area, which were previously separated from the bedrock and fell to the slopes, by breaking or burying them during construction. In this area where rock blocks with a risk of falling are still observed, it is thought that the risk of rock fall can be eliminated by applying engineering measures such as diking at the foot of the rock slopes, building retaining structures, and applying dense forestation and fencing on the slopes.

REFERENCES

Abidin, M. H. Z., Saad, R., Ahmad, F., Wijeyesekera, D. C., Baharuddin, M. F. T., 2012. Seismic refraction investigation on near surface landslides at the Kundasang area in Sabah, Malaysia. Procedia Engineering, 50, 516-531.

Al-Saigh, N. H., AL-Dabbagh, H., 2010. Identification of landslide slip-surface and its shear strength: A new application for shallow seismic refraction method. Journal Geological Society of India, 76, 175-180.

Arndt, R., Römer, A., Sendlhofer, G., Restner, U., 2000. Geophysical reconnaissance methods for landslides in soft rocks. Internationals Symposium Interprevent, Villach / Österreich, 191-201.

Batayneh, A. T., Al Diabat, A. A., 2002. Application of a 2-D electrical tomography technique for investigating landslides along the Amman-Dead Sera Highway, Jordan. Env. Geology, 42, 399-403.

Bernstone C., Dahlin T., Ohlsson T., Hogland W., 2000. DC-resistivity mapping of internal landfill structures: two pre-excavation surveys. Env. Geol., 39 (3-4): 360-371.

Bichler A., Bobrowsky P., Best M., Douma M., Hunter J., Calvert T., Burns R., 2004. Three-dimensional mapping of a landslide using a multi-geophysical approach: the Quesnel Forks landslide. Landslides, 1, 29-40.

Bieniawski, Z. T., 1975. The point-load test in geotechnical practice. Engineering Geology, 9, 1-11.

Bogoslovsky V. A., Ogilvy A. A., 1977. Geophysical methods for the investigation of landslides. Geophysics, 42, 562-571.

Brooke, J. P., 1973. Geophysical investigation of a landslide near San Jose, California, Geoexploration, 11 (2), 61-73.

BSSC (Building Seismic Safety Council)., 1997. NEHRP recommended provisions for Seismic Regulations for New Buildings and Other Structures. Part I, Provisions (FEMA 302), 334.

Campbell, R. B., Bower, C. A., Richards, L. A., 1948. Change of electrical conductivity with temperature and the relation of osmotic pressure to electrical conductivity and ion concentration for soil extracts. Soil Sci. Soc. Am. Proc., 13, 66-69.

Candansayar, M. E., Basokur, A. T., 2001. Detecting small-scale targets by the 2D inversion of two-sided three-electrode data: application to an archaeological survey. Geophysical Prospecting, 49 (1), 40-53.

Constable, S. C., Parker, R. L., Constable, C. G., 1987. Occam's inversion: A practical algorithm for generating smooth models from electromagnetic sounding data. Geophysics, 52, 289–300.

Cummings, D., Clark, B. R., 1988. Use of seismic refraction and electrical resistivity surveys in landslide investigations. Bulletin of the Association of Engineering Geologists, XXV (4), 459-464.

Chen, F. H., 1975. Foundations on expansive soils: Developments in geotechnical engineering 12, Elsevier Scientific, New York.

Choobbasti, A. J., Rezaei, S., Farrokhzad, F., 2013. Evaluation of site response characteristics using microtremors. Gradevinar, 65 (8), 731-741.

Crawford, M. M., Zhu, J., Webb, S. E., 2015. Geologic, geotechnical, and geophysical investigation of a shallow landslide, eastern Kentucky. Environmental & Engineering Geoscience, 21 (3), 181-195.

Çoruh, T., 1991. Biostratigraphy and paleogeographic evolution of the Campanian-Tanesian sequence surfaced around Adıyaman (northwest of XI Region and XII Region). Research Center, Report No: 1656, 101.

Dahlin, T., 1996. 2D Resistivity surveying for environmental and engineering applications. First Break, 14, 275-284.

Dahlin, T., Bernstone, C., 1997. A roll-along technique for 3D resistivity data acquisition with multi-

electrode array, in Proceedings of SAGEEP, R. S. Bell (Editor), EEGS, March, 1997, Reno, Nevada, 2, 927-935.

Dahlin, T., Zhou, B., 2004. A numerical comparison of 2-D resistivity imaging with 10 electrode arrays. Geophysical Prospecting, 52, 379-398.

Deere, D. U., Miller, R. P., 1966. Engineering classification and index properties for intact rock. Air Force Weapons Laboratory Technical Report, Volume I-II, Leonard Hill, 270.

Drahor, M. G., Göktürkler, G., Berge, M. A., Kurtulmuş, T. Ö., 2006. Application of electrical resistivity tomography technique for investigation of landslides: a case from Turkey. Environmental Geology, 50, 147–155.

Frasheri, A., Kapllani, L., Dhima, F., 1998. Geophysical landslide investigation and prediction in the hydrotechnical works. Journal of the Balkan Geophysical Society, 1 (3), 38-43.

Gelişli, K., 2018. Geophysical methods for the investigation of landslides. Journal of Applied Earth Sciences, 17 (2), 115-126. doi: 10.30706/uybd.458107

Göktürkler, G., Balkaya, Ç., Erhan, Z., 2008. Geophysical investigation of a landslide: The Altındağ Landslide Site, İzmir (Western Turkey). Journal of Applied Geophysics, 65, 84-96.

Gürbüz, M., Koç, N., Hamzaçebi, G., 2005. Studying the structure of landslides with geophysical approaches. Earthquake Symposium, 23-25 March, Kocaeli, 1154-1156.

Gupta, A. S., Rao, K. S., 1998. Index properties of weathered rocks: inter-relationships and applicability. Bulletin of Engineering Geology and the Environment, 57, 161-172.

Griffiths, D. H., Turnbull, J., 1985. A multi-electrode array for resistivity surveying, First Break, 3 (7), 16-20.

Griffiths, D. H., Turnbull, J., Olayinka, A. I., 1990. Two-dimension resistivity mapping with a computer controlled array. First Break, 8 (4), 12l-129.

Havenith, H. B., Jongmans, D., Abdrakmatov, K., Trefois, P., Delvaux, D., Torgoev, A., 2000. Geophysical investigations on seismically induced surface effects, case study of a landslide in the Suusamyr valley, Kyrgyzstan. Survey in Geophysics, 21, 349-369.

Holtz, W. G., Gibbs, H. J., 1956. Engineering properties of expansive clays. Transactions of the American Society of Civil Engineers, 121 (1), 641-677.

ISRM., 1978. Suggested methods for the quantitative description of discontinuities in rock masses, Int. J. Rock. Mechn. and Mining Sei. and Geomech, Abstr., 15 (6), 319-368.

Jongmans D., Garambois S., 2007. Geophysical investigation of landslides: a review. Bulletion De La Societe Geologique De France, 178 (2), 101-112.

Jongmans, D., Bievre, G., Renalier, F., Schwartz, S., Beaurez, N., Orengo, Y., 2009. Geophysical investigation of a large landslide in glaciolacustrine clays in the Trieves area (French Alps). Engineering Geology, 109, 45-56.

Jusoh, H., Osman, S. B. S., 2017. The correlation between resistivity and soil properties as an alternative to soil investigation. Indian Journal of Science and Technology, 10 (6), 1-5. doi: 10.17485/ijst/2017/ v10i6/111205.

Karslı, H., 2015. Geophysical methods and application examples in landslides investigations. Prof. Dr. Ali Keçeli Geophyscis-Geotechnical Workshop Proceedings, 51-60.

Karslı, H., Şenkaya, M., Şenkaya, G, V., Kirici, M., 2018. Integrated applications of geophysical methods and importance of multidimensional imaging in landslide investigation, 2nd landslide symposium HEYSEMP, Book of Absract, 27-28.

Larsen, S., Widdowson, A. E., 1965. Determination of soil moisture by electrical conductivity. Soil Sci. 101, 420.

Lapenna, V., Lorenzo, P., Perrone, A., Piscitelli, S., Rizzo, E., Sdao, F., 2003. High-resolution geoelectrical tomographies in the study of the Giarrossa landslide (Potenza, Basilicata). Bull. Eng. Geol. Env., 62, 259-268.

Lebourg, T., Binet, S., Tric, E., Jomard, H., El Bedoui, S., 2005. Geophysical survey to estimate the 3D sliding surface and the 4D evolution of the water pressure on part of a deep-seated landslide. Terra Nova, 17, 399-406.

Li, Y., Oldenburg, D. W., 1992. Approximate inverse mapping in DC resistivity problems. Geophysical Journal International, 109, 343-362.

Ling, C., Xu, Q., Zhang, Q., Ran, J., Lv, H., 2016. Application of electrical resistivity tomography for investigating the internal structure of a translational landslide and characterizing its groundwater circulation (Kualiangzi landslide, southwest China). Journal of Applied Geophysics, 131, 154-162.

Loke, M. H., Barker, R. D., 1996a. Rapid least square inversion of apparent resistivity pseudosections by

a quasi-Newton method. Geophysical Prospecting, 44 (1), 131–152. doi:10.1111/j.13652478.1996.tb00142.x

Loke, M. H., Barker, R. D., 1996b. Pratical techniques for 3D resistivity surveys and data inversion. Geophysical Prospecting, 44 (3), 499-523. doi:10.1111/j.1365-2478.1996.tb00162.x

Lopes, I., Santos, J. A., Gomes, R. C., 2014. Vs profile: measured versus empirical correlations-a Lower Tagus river valley example. Bulletin of Engineering Geology and the Environment, 73 (4), 1127-1139.

Merritt, A. J., Chambers, J. E., Murphy, W., Wilkinson, P. B., West, L. J., Gunn, D. A., Meldrum, P. I., Kirkham, M., Dixon, N., 2014. 3D ground model development for an active landslide in Lias mudrocks using geophysical, remote sensing and geotechnical methods. Landslides, 11 (4), 537-550.

Mondal, S. K., Sastry, R. G., Pachauri, A. K., Gautam, P. K., 2008. High resolution 2D electrical resistivity tomography to characterize active Naitwar Bazar landslide, Garhwal Himalaya, India: Current Science, 94, 871–875.

Otto, J. C., Sass, O., 2006. Comparing geophysical methods for Talus Slope investigations in the Turtmann Valley (Swiss Alps). Geomorphology, 76, 257-272.

Özcep, F., Tezel, O., Asci, M., 2009. Correlation between electrical resistivity and soil-water content: Istanbul and Golcuk. International Journal of Physical Sciences, 4 (6), 362-365.

Özcep, F., Yıldırım, E., Tezel, O., Asci, M., Karabulut, S., 2010. Correlation between electrical resistivity and soil-water content based artificial intelligent techniques. International Journal of Physical Sciences, 5 (1), 47-56.

Özcep, F., Erol, E., Saraçoğlu, F., Haliloğlu, M., 2012. Seismic landslide analysis: Gurpinar (Istanbul) as a case history. Environ Earth Sci., 66, 1617–1630.

Palmer D. F., Weisgarber, S. L., 1988. Geophysical survey of the Stumpy Basin landslide, Ohio. Bulletin of the Association of Engineering Geologists, XXV (3), 363-370.

Pozdnyakova, L. A., Pozdnyakov, A. I., Karpachevsky, L. O., 1996. Study hydrology of valley agricultural landscapes with electrical resistance methods. In: Proceeding of XXI Assembly of European Geophysical Society, HS16 "The Hydrology of Small Agricultural Catchments". The Hague, Netherlands, 341-352.

Pozdnyakova, L. A., 1999. Electrical Properties of Soils. Ph.D. Thesis, University of Wyomins, USA.

Ravindran, A., Ramanujam, N., 2012. Palaeoscars and landslide prediction using 2D ERI techniques in Ooty Area, Nilgiri District, Tamilnadu. Archives of Applied Science Research, 4 (1), 262-268.

Rezaei, S., Shooshpasha, I., Rezaei, H., 2018. Evaluation of landslides using ambient noise measurements (Case Study: Nargeschal landslide). International Journal of Geotechnical Engineering, doi:10.1080/19386362.2018.1431354.

Rezaei, S., Shooshpasha, I., Rezaei, H., 2018. Empirical correlation between geotechnical and geophysical parameters in a landslide zone (Case Study: Nargeschal Landslide), Earth Sciences Research Journal, Earth Sci. Res. J., 22 (3), 195-204.

Ristic, A., Abolmasow, B., Govedarica, M., Petrovacki, D., Ristic, A., 2012. Shallow landslide spatial structure interpretation using a multi-geophysical approach. Acta Geotechnica Slovenica, 1, 47-59.

Rhoades, J. D., Van Schilfgaarde, J., 1976. An electrical conductivity probe for determining soil salinity. Soil Sci. Soc. Am. J., 40, 647-650.

Rhoades, J. D., Shouse, P. J., Alves, W. J., Manteghi, N. A., Lesch, S. M., 1990. Determining soil salinity from soil electrical conductivity using different models and estimates. Soil Sci. Soc. Am. J., 54, 46-54.

Sass O., Bell R., Glade T., 2008. Comparison of GPR, 2D-resistivity and traditional techniques for the subsurface exploration of the Öschingen landslide, Swabian Alb (Germany). Geomorphology, 93, 89-103.

Sil, A., Haloi, J., 2017. Empirical correlations with standard penetration test (SPT)-N for estimating shear wave velocity applicable to any region. International Journal of Geosynthetics and Ground Engineering, 3 (3), 22.

Soto, J., Galve, J. P., Palenzuela, J. A., Azañón, J. M., Tamay, J., Irigaray, C., 2017. A multi-method approach for the characterization of landslides in an intramontane basin in the Andes (Loja, Ecuador). Landslides, 14 (6), 1929-1947. doi: 10.1007/s10346-017-0830-y.

Sungurlu, O., 1974. The geology of the north fields of the VI. Region, Declarations of 2nd Turkish Petroleum Congress. 22 25 January, Ankara, 85-107.

Syed Baharom Syed, O., Mohammad, N. F., Fahad, I. S., 2014. Correlation of electrical resistivity with

some soil parameters for the development of possible prediction of slope stability and bearing capacity of soil using electrical parameters. Pertanika Journal Scince and Technology, 22 (1), 139-152.

Szokoli, K., Szarka, L., Metwaly, M., Kalmár, J., Prácser, E., Szalai, S., 2017. Characterisation of a landslide by its fracture system using electric resistivity tomography and pressure probe methods. Acta Geodaetica et Geophysica, 53 (1), 15-30. doi: 10.1007/s40328-017-0199-3.

Şenkaya, G, V., Şenkaya, M., Karslı, H., Güney, R., 2020. Integrated shallow seismic imaging of a settlement located in a historical landslide area. Bulletin of Engineering Geology and the Environment, 79 (4), 1781-1796. doi: 10.1007/s10064-019-01612-0.

TBDY., 2018. Turkey earthquake building regulations. Ankara: Disaster and Emergency Management Presidency.

Thokchom, S., Rastogi, B. K., Dogra, N. N., Pancholi, V., Sairam, B., Bhattacharya, F., Patel, V., 2017. Empirical correlation of SPT blow counts versus shear wave velocity for different types of soils in Dholera, western India. Natural Hazards, 86 (3), 1291-1306.

Ullah, I., Prado, R. L., 2017. Soft sediment thickness and shear-wave velocity estimation from the H/V technique up to the bedrock at meteorite impact crater site, Sao Paulo city, Brazil. Soil Dynamics and Earthquake Engineering, 94, 215-222.

Uyanık, O., Türker, E., 2007. Fethiye Eşen technical properties and interpretation of potential landslide in II HES switch and power plant site. Süleyman Demirel University Journal of Science Institute, 11 (1), 84-90.

Uyanık, O., Çatlıoğlu, B., 2014. Determination of landslide geometry by using electrical resistivity and seismic refraction method, Süleyman Demirel University. Journal of Natural and Applied Science, 18 (3), 22-29.

Uyanık, O., Sabbağ, N., 2013. Determination of landslide geometry by geophysical methods, 4th International Geosciences Student Conference, 25-29 April, Paper ID: 1587 Berlin/Germany.

Van Overmeeren, R. A., Ritsema, I. L., 1988. Continuous vertical electrical sounding. First Break, 6 (10), 313–324.

Wisen R., Auken E., Dahlin T., 2005. Combination of 1D laterally constrained inversion and 2D smooth inversion of resistivity data with a priori data from boreholes. Near Surf. Geophys, 3, 71-79.

Yılmaz, S., Narman, C., 2015. 2-D electrical resistivity imaging for investigating an active landslide along a ridgeway in Burdur region, southern Turkey. Arabian Journal of Geosciences, 8 (5), 3343-3349.

Yordkayhun, S., Sujitapan, C., Chalermyanont, T., 2014. Joint analysis of shear wave velocity from SH-wave refraction and MASW techniques for SPT-N estimation. Songklanakarin Journal of Science and Technology, 36, 333-344.

https://www.agiusa.com

https://www.mta.gov.tr

http://www.seistronix.com/